Joint Active and Passive Microwave Thermometry of Ice Sheets

Anna L. Broome, *Graduate Student Member, IEEE*, Dustin M. Schroeder, *Senior Member, IEEE*, and Joel T. Johnson, *Fellow, IEEE*

***Abstract*— Measurement of ice-sheet thermal state via microwave remote sensing techniques has the potential to provide critically needed observations on englacial temperature at the local and continental scale. Better constraints of the vertical englacial temperature structure are needed to improve understanding of thermomechanical processes, ice rheology, and basal sliding, and to reduce uncertainty in interpretations of basal conditions such as material, roughness, and thermal state. We investigate the potential to combine active and passive microwave remote sensing techniques, namely ice-penetrating radar sounding and microwave radiometry, to enable more precise, accurate, and robust measurement of ice-sheet thermal state across widely varying thermal regimes. We simulate the effects of englacial temperature profiles on the attenuation and brightness temperature and explore the performance tradeoffs for joint radar-radiometer system architectures. Our analysis shows that active and passive microwave measurements have complementary sensitivities to englacial temperature as a function of depth, and that a ground-based joint radar-radiometer system can reduce the requirements and complexity demanded of each single instrument.**

***Index Terms*— Ice-penetrating radar, microwave radiometry, radar remote sensing, radar sounding.**

I. Introduction

ICE-sheet thermal state is one of the most consequential and one of the most poorly known physical parameters involved in our understanding and modeling of ice flow and dynamics. Englacial temperature affects ice rheology [1], internal deformation [2], and basal sliding [3], [4]. It also encodes information on the geothermal heat flux (GHF), an important influence on basal melting and ice flow [5], [6]. Current measurements of ice-sheet thermal state are severely limited in terms of their spatial and temporal coverage, as well as their accuracy. These limitations contribute to significant uncertainties in projections of ice-sheet behavior and sea level change derived from numerical ice-sheet models. Better (larger spatial scale, more frequent, more accurate, and more precise) observations of ice-sheet thermal state (englacial temperature) are needed to constrain and improve understanding of thermomechanical processes and feedback mechanisms used in large-scale numerical ice-sheet models [7], [8].

Current methods for direct observation of ice-sheet thermal state include instrumenting boreholes (typically shallow) and deep ice cores [9]. Unfortunately, these techniques are spatially and temporally sparse, with fewer than 25 ice cores drilled to bedrock in total across Greenland and Antarctica [10], [11], [12]. They are also extremely resource intensive. To obtain observations of ice-sheet thermal structure over a larger area, the community has turned to microwave remote sensing instruments, specifically ice-penetrating radar sounders [13], [14] and microwave radiometers [15]. Ice-penetrating radar sounders used for studying polar ice sheets are typically chirped radar systems that transmit frequency-modulated pulses of electromagnetic energy and measure the power reflected from various dielectric interfaces within the ice (echo power), including englacial layers and the ice-sheet bed [16]. Englacial temperature is the primary variable affecting attenuation of electromagnetic signals through ice [17], and ice-penetrating radar measurements of echo power are sensitive to englacial conditions, including ice temperature, as well as basal conditions, including material, roughness, and thermal state [18]. Microwave radiometers measure a combination of thermal emissions originating within the ice sheet and from the bed, with each emission contribution related to the local physical temperature and experiencing attenuation while propagating to the ice surface [19]. The combined emissions observed are reported as a brightness temperature, which can then be related to the physical temperature of the ice sheet [20].

Ice-penetrating radar sounders and microwave radiometers are both sensitive to the physical temperature of ice sheets, but each technique has distinct limitations when used in the context of observing ice-sheet thermal state and basal conditions. Relating brightness temperature to physical temperature is typically done using a "model-based retrieval" [15], [21]. This retrieval process a priori assumes a functional form of the thermal profile as a function of depth. The expected brightness temperature is then forward modeled for a set of thermal profiles with the assumed functional form. Measurements of brightness temperature are compared to the forward model, and the retrieved englacial temperature is determined by finding the best match between the forward model and measurements. While this type of retrieval does provide an estimate of the thermal structure of the ice sheet based on microwave emissions, it requires assumptions on the form of the thermal profile that may prevent its application in many of the areas most critical for understanding and projecting

Manuscript received 29 October 2022; revised 22 February 2023; accepted 6 March 2023. Date of publication 10 March 2023; date of current version 21 March 2023. This work was supported in part by the Heising-Simons Foundation and in part by the National Defense Science and Engineering Graduate (NDSEG) Fellowship Program. *(Corresponding author: Anna L. Broome.)*

Anna L. Broome is with the Department of Electrical Engineering, Stanford University, Stanford, CA 94305 USA (e-mail: abroome@stanford.edu).

Dustin M. Schroeder is with the Department of Electrical Engineering and the Department of Geophysics, Stanford University, Stanford, CA 94305 USA.

Joel T. Johnson is with the ElectroScience Laboratory, The Ohio State University, Columbus, OH 43210 USA.

Digital Object Identifier 10.1109/TGRS.2023.3255219

ice-sheet behavior, evolution, and contribution to sea level.

Several satellite and airborne radiometer missions have been used to study the thermal properties of Earth's ice sheets. For example, using 1.4 GHz brightness temperature measurements from the Soil Moisture Active and Passive (SMAP) satellite, the presence of meltwater and the location of firn aquifers in Greenland has been mapped [22]. The 1.4 GHz brightness temperature measurements of the Soil Moisture and Ocean Salinity (SMOS) satellite have been used to estimate temperature profiles in Antarctica [21]. The retrieval algorithm in [21] uses the Robin model for englacial temperature and is therefore limited to areas where the Robin model is valid, primarily the cold, deep interior of the Antarctic Ice Sheet [6]. SMOS observations of brightness temperature in Antarctica are also limited by the relatively high frequency (1.4 GHz) of the radiometer, which may be insensitive to thermal emissions from deeper within the ice, and from the bed material, which are highly attenuated before reaching the surface. Estimating deep englacial temperatures and basal conditions from this system thus require significant extrapolation, notably increasing uncertainty at depth [21].

The Ultra-wideband Software-Defined Microwave Radiometer (UWBRAD) is an airborne instrument that seeks to overcome the limited depth-sensitivity of radiometers like SMOS by utilizing 12 channels across the 500–2000 MHz band to measure ice-sheet brightness temperature [23]. The processing of UWBRAD multi-frequency brightness temperature measurements to date has also followed a model-based retrieval using the Robin model for ice-sheet temperature [15]. The existing method therefore also does not provide englacial temperature measurements in glaciologically critical areas, including those with fast-flowing ice, those that are not in a steady state, those with temperate ice, or those areas with thermal profiles that cannot be described by analytic models. The extended bandwidth of UWBRAD leverages a frequency-dependent depth sensitivity to temperature, with its lower frequencies more sensitive to deeper portions of the ice column and higher frequencies more sensitive to upper portions of the ice column [20]. While the extension to lower frequencies improves temperature retrievals at depth, deep and/or warm englacial temperatures as well as basal conditions remain challenging to observe.

A frequency-dependent sensitivity to temperature versus depth arises from the frequency dependence of electromagnetic attenuation in ice, which is primarily evident at frequencies above 500 MHz [24]. Because most ice-penetrating radar sounders operate beneath 500 MHz, where attenuation is approximately frequency independent, a similar multi-frequency analysis of radar sounding data does not provide additional information on attenuation, or temperature, as a function of depth (it does however provide valuable data on basal roughness [25]). Because ice-penetrating radar sounders are designed to observe reflections from the ice-bed interface and to probe the full depth of the ice column, a radar measurement of the total two-way attenuation emphasizes the increased attenuation associated with the warmer temperatures near the bed.

To investigate basal conditions using ice-penetrating radar sounders requires correcting for attenuation, which can otherwise cause significant ambiguity in the interpretation of basal echo powers [26]. Correcting for attenuation in radar sounding data requires the use of ancillary data from nearby ice cores [27], the use of a thermomechanical model [28], [29], analysis of englacial layer reflectivity [30], [31], or adaptive correction using basal echoes [13], all of which require additional assumptions on the englacial and basal conditions. Because attenuation is primarily a function of temperature, improved understanding and observations of englacial temperature are thus also useful for correcting attenuation in radar sounding data and enabling more precise and accurate measurements of ice-sheet basal conditions [25], [32]. More accurate measurements of englacial attenuation will also enable higher fidelity analysis of englacial water content [33] and basal accretion rates [34].

Even at the level of these general descriptions, it is clear that radar sounders and radiometers probe the thermal state of ice sheets in distinct and potentially complementary ways. Here, we explore that complementarity in the context of instrument architectures for a ground-based, multi-frequency joint radar-radiometer instrument for measuring the subsurface thermal structure of ice sheets. In this article, we show that englacial temperatures can be observed with greater fidelity by combining active and passive microwave measurements from ice-penetrating radar sounders and microwave radiometers. This has the potential not only to improve microwave thermometry at the glacier to ice-sheet scale, but also to improve studies of basal conditions using basal reflectivity. Because the underpinnings of a radar receiver and radiometer are nearly identical, they can be combined into a single, joint instrument that is optimized for measuring thermal properties. Here we explore the relative performance of each instrument alone and in combination and discuss their ability to improve remote sensing of englacial temperatures. Section II introduces the physical models we use for our analysis, and Section III details our simulation framework. In Sections IV and V, we discuss the improvements a joint system enables from the radar and radiometer analysis perspectives, respectively. In Section VI we explore the requirements on each instrument's performance that dictate the architectural tradeoffs and decisions relevant to implementation in a joint ground-based system, while Section VII provides concluding remarks.

II. Physical Models

In order to explore the relative performance of radars and radiometers for measuring englacial temperature within the ice sheet, we simulate the effect of englacial temperature on attenuation and brightness temperature. Using a general model for englacial temperature allows us to explore the sensitivity of various system architectures to a wide range of physically plausible temperature profiles. The classic Robin model [35], which is commonly used in model-based retrievals of ice-sheet temperature [15], [21], [36] cannot be applied in some of the most interesting and important areas of ice sheets relevant for understanding and modeling ice-sheet evolution and stability (e.g., fast-flowing regions with non-zero horizontal advection) [6], [37]. To explore a wider range of thermal profiles, we extend our englacial temperature model to include the Budd column model, which accounts for moderate horizontal advection of ice [38], in addition to the Robin model. It is straightforward to adapt our analysis approach to utilize other thermomechanical or numerical ice-sheet models as well (e.g., [39], [40]). For englacial attenuation, we use

TABLE I
PARAMETERS USED FOR ENGLACIAL TEMPERATURE SIMULATION

Variable	Parameter	Values (Step Size)
$T(z)$	temperature as function of depth	–
T_s	surface temperature	213.15–273.15 (5) K
GHF	geothermal heat flux	10–120 (5) mW/m^2
β_b	GHF plus integrated strain heating	10–120 (5) mW/m^2
$\dot{b}_i$	surface mass balance rate	0.005–3 (0.1) m/yr
H	ice thickness	1000, 3000 m
λ	lapse rate	-0.01 K/m
α	surface slope	-1–0° (0.25°)
$\bar{u}$	average surface velocity	0, 1, 10, 50, 100, 500, 1000 m/yr
k_t	ice thermal conductivity	2.25 W/m/K
κ	ice thermal diffusivity	37.2 m^2/yr

the semi-empirical Matzler model [24] that encompasses the wide range of frequencies used for simulating attenuation and brightness temperature. Finally, our brightness temperature model is a generic incoherent cloud model [41], which is commonly used in the radiometer ice-sheet retrieval literature [20]. In this section, we walk through the basics behind each of these models.

A. Englacial Temperature Model

Our model space for englacial temperatures encompasses the traditional Robin model, which describes thermal profiles in areas of the ice sheet with negligible horizontal advection and negligible strain heating plus a simple analytic temperature model, the Budd column model, which allows for moderate horizontal advection and strain heating at the bed [42].

The steady-state Robin temperature model describes the englacial temperature $T(z)$ at depth z as

$$T(z) = T_s - z_* \frac{\sqrt{\pi}}{2} \frac{\text{GHF}}{k_t} \left[\text{erf}\left(\frac{z}{z_*}\right) - \text{erf}\left(\frac{H}{z_*}\right) \right] \quad (1)$$

where $T_s = T(z = H)$ is the temperature at the surface of the ice, GHF is the geothermal heat flux, k_t is the ice thermal conductivity, ${z_*}^2 = 2\kappa H/\dot{b}_i$ is defined for convenience, κ is the ice thermal diffusivity, H is the total ice thickness, and $\dot{b}_i$ is the surface mass balance rate (often called the accumulation rate) [35]. The Budd column model for $T(z)$ in contrast states

$$T(z) = T_s - z_* \beta_b \frac{\sqrt{\pi}}{2} \left[\text{erf}\left(\frac{z}{z_*}\right) - \text{erf}\left(\frac{H}{z_*}\right) \right] - \frac{2\bar{u}\alpha\lambda H}{\dot{b}_i} \left[E\left(\frac{H}{z_*}\right) - E\left(\frac{z}{z_*}\right) \right] \quad (2)$$

where β_b is the GHF plus integrated strain heating, α is the surface slope, λ is the lapse rate, and $\bar{u}$ is the average horizontal velocity [38]. The parameters T_s, H, κ, z_*, and $\dot{b}_i$ are the same as above. Values for all physical parameters used in our simulations are listed in Table I. In (1) and (2), erf represents the error function. Budd et al. [38] defines $E(x)$ as the integral of Dawson's integral, given by

$$E(x) = \int_0^x \left[\text{e}^{-y^2} \int_0^y \text{e}^{t^2} dt \right] dy. \quad (3)$$

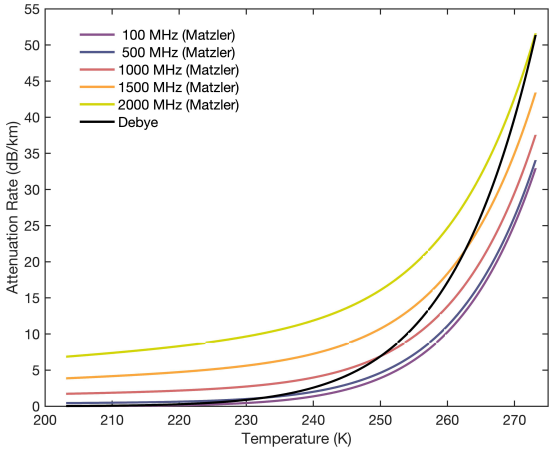

Fig. 1. Attenuation rate as a function of temperature using the frequency independent Debye model and the Matzler model at different frequencies.

B. Englacial Attenuation Model

The attenuation of an electromagnetic signal through ice is primarily dependent on the physical temperature of the ice but is also influenced by ice chemistry and electromagnetic frequency [24], [30]. Attenuation is quantified via the absorption coefficient, κ_α, defined as

$$\kappa_\alpha(T, f) = \frac{2\pi}{\lambda_0} \frac{\epsilon''_{\text{ice}}(T, f)}{\sqrt{\epsilon'_{\text{ice}}}} \quad (4)$$

where $\epsilon_{\text{ice}} = \epsilon'_{\text{ice}} + j\epsilon''_{\text{ice}}(T, f)$ is the ice dielectric constant, $j = \sqrt{-1}$, and λ_0 is the signal wavelength in air. The total two-way attenuation in dB experienced by a radar signal that reflects off the bed is

$$L_{\text{att}}\ [\text{dB}] = \int_0^H 2\kappa_\alpha(T, f) 10 \log_{10}(e) dz \quad (5)$$

where e is Euler's number.

Traditionally, ice-penetrating radar sounders have assumed the frequency dependence of attenuation to be negligible within their typical frequency range (1–300 MHz) [17]. This assumption is grounded in the Debye model for the dielectric constant of ice, which assumes a single relaxation in the hertz to kilohertz range [24]. While the Debye model is used widely within the ice-penetrating radar community, it does not support the frequency range needed for radiometry on ice sheets. Instead, the ice-sheet radiometer literature typically utilizes the semi-empirical Matzler model for ϵ'' that includes explicit frequency and temperature dependencies [24], [43]. At frequencies less than 500 MHz and for low temperatures, the Matzler and Debye models match relatively well as shown in Fig. 1. It is also evident in Fig. 1 that the Matzler model exhibits little frequency dependence beneath 500 MHz. At higher frequencies, the Matzler model exhibits a more pronounced frequency dependence. In this article, we exclusively use the Matzler model as detailed in [43] and a real permittivity of $\epsilon'_{\text{ice}} = 3.17$ to encompass the wide range of frequencies needed for both the radar and radiometer instrument simulations. Using the Matzler model does not prevent simulations of radar attenuation, whereas using the Debye model would result in a loss of information for the simulations of radiometer brightness temperature.

C. Brightness Temperature Model

We model brightness temperature following the "cloud" model in [20], which integrates the thermal emission from discrete layers of ice, accounting for attenuation at each layer, as well as the reflection and transmission coefficients of the ice-bed interface and the ice-surface interface. Internal reflections within the ice column and scattering are neglected in this model.

The resulting brightness temperature is

$$\begin{aligned} &T_b(\theta,\phi) \\ &= (1-\Gamma_{\text{surf}}(\theta)) \\ &\left[\int_0^H T(z)\kappa_\alpha(z)\frac{1}{\cos(\theta)}\exp\left(-\int_z^H \kappa_\alpha(z')\frac{1}{\cos(\theta)}dz'\right)dz\right. \\ &\left.+(1-\Gamma_{\text{bed}}(\theta))\ T(0)\exp\left(-\int_0^H \kappa_\alpha(z)\frac{1}{\cos(\theta)}dz\right)\right] \end{aligned} \quad (6)$$

where Γ_{surf} is the surface Fresnel power reflection coefficient, Γ_{bed} is the bed Fresnel power reflection coefficient, $T(z)$ is the physical temperature of the ice, $\kappa_\alpha(z)$ is the absorption coefficient of the ice, H is the ice thickness, and θ is the angle off nadir. $T(0)$ is the temperature at the ice-bed interface. For all analyses, reflection coefficients are computed for horizontal polarization [19], and assume a permittivity of $2.63 - j0.046$ (frozen rock, [25]) at the ice-sheet base. The above description neglects reflections in the upper layers of the ice sheet caused by density variations in the firn [44]. While these effects can be significant, they are not related to englacial temperature sensitivities of primary interest in this work. It is noted that radar observations have the potential to provide information on firn layering effects on the radiometer, so combined radar and radiometer measurements are also of interest for this application [45], [46], [47], [48], [49].

The pattern-integrated brightness temperature takes into account the beam pattern of the radiometer antenna and is given by

$$T_A{}' = \frac{\int\int_{4\pi} T_B(\theta,\phi)\ F(\theta,\phi)\ d\Omega}{\int\int_{4\pi} F(\theta,\phi)\ d\Omega} \quad (7)$$

where $T_B(\theta,\phi)$ is the brightness temperature distribution of the observed scene, $F(\theta,\phi)$ is a normalized antenna radiation pattern, and $d\Omega$ is the differential solid angle [19]. The brightness temperature is assumed to be spatially uniform for the purposes of our simulations.

III. Temperature Sensitivity Simulation

To investigate the complementary sensitivities of radars and radiometers to ice-sheet thermal structure, we develop a basic simulation of attenuation and brightness temperature responses to different thermal profiles. We use this simulation to understand how different system architectures influence thermal sensitivity. Our simulation involves computing a superset of plausible temperature profiles from the Robin and Budd models described in Section II-A. Plausible temperature profiles are produced from each model by sweeping over the parameter ranges shown in Table I under the assumptions that:

1) the temperature anywhere within the ice column cannot exceed the melting point (273.15 K);
2) the temperature anywhere within the ice column cannot be beneath 203.15 K.

If a profile does not meet these assumptions, it is considered nonphysical and discarded from the superset. For each profile in the superset, we calculate the observed brightness temperature and attenuation for frequencies ranging from 200 MHz to 2 GHz. In total, we simulated 669 660 thermal profiles, of which 358 667 were considered plausible and included in the superset.

We select thermal profiles from the superset to represent various ice-sheet thermal regimes for forward modeling (e.g., cold-bedded areas, warm-bedded areas, slow-flowing areas, fast-flowing areas, and areas with/without a significant horizontal advection signature). We evaluate system architectures by specifying instrument frequencies and radiometric resolution for both the radiometer and the radar. We then calculate brightness temperature and attenuation measurements for the true profile and a specified system. Based on these brightness temperature and attenuation values, we find the subset of temperature profiles that are consistent with the measurements. A profile is considered consistent if the brightness temperature and/or attenuation the instrument observes is within the radiometric resolution of the measurements produced by the true profile and if its surface temperature is within ± 5 K of the true value. The latter process acknowledges the fact that profiles having consistent brightness temperatures but larger differences in surface temperatures could be rejected using surface temperature data from a climate model (e.g., [50]) or via a co-located infrared camera [51]. We note that seasonal temperature variations at the surface are typically not observable beneath depths of 20 m [35] and our simulations are representative of mean annual temperature profiles. We investigate the relative and combined performance of active and passive observations by determining the matching profile subsets for radiometer brightness temperature measurements alone, radar attenuation measurements alone, and radar and radiometer measurements in combination. In what follows, the difference among consistent temperature profiles at a given depth will be described as the temperature retrieval error for a given system. We note that this definition does not involve the direct application of a retrieval method but instead emphasizes the sensitivity of the observed quantity to the temperature at a specific depth. For a combined radiometer-radar system, consistent profiles must provide both brightness temperatures and attenuation measurements within the specified instrument sensitivities.

To visualize the temperature sensitivity as a function of depth we use stacked box and whisker plots showing the difference in temperature between the true and matching profiles as a function of depth. An example of this visualization is shown in Fig. 2(b). Throughout this article, the red line in these plots represents the median temperature retrieval error, the dark blue regions represent the 25th–75th percentile temperature error, the light blue the 3σ temperature error, and the gray dots show the outliers. A perfect temperature retrieval throughout the ice column would have a single red vertical line at 0 K temperature error.

IV. Improving Attenuation Constraints in Radar Data

Disentangling the effects of attenuation and basal conditions in ice-penetrating radar data has the potential to greatly reduce uncertainty in interpretations of basal thermal state,

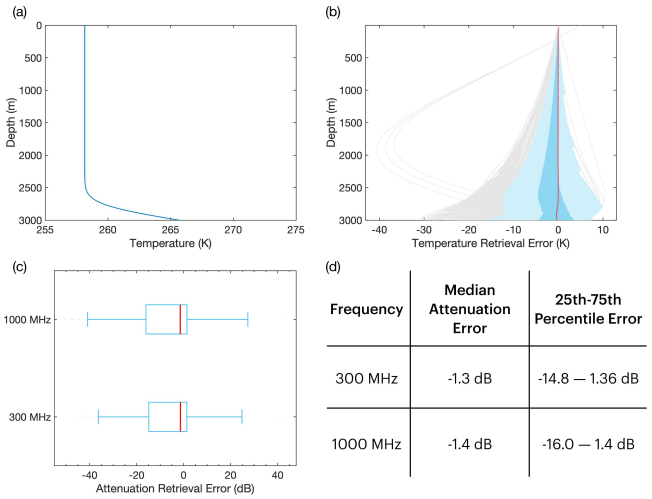

Frequency	Median Attenuation Error	25th-75th Percentile Error
300 MHz	-1.3 dB	-14.8 — 1.36 dB
1000 MHz	-1.4 dB	-16.0 — 1.4 dB

Fig. 2. (a) Simulated true temperature profile. (b) Simulated temperature retrieval errors produced by a radiometer operating at 300 and 1000 MHz with ±1 K radiometric resolution. Less than 0.5 K absolute median error throughout the entire depth of the ice column. (c) and (d) Corresponding error in attenuation at 300 and 1000 MHz, calculated from the thermal profiles in (b). In (c) radar attenuation performance is represented by a standard box and whisker plots with the -3σ, 25th percentile, median, 75th percentile, and $+3\sigma$ values and outliers indicated.

material, and roughness [18], [26]. However, disentangling these effects is quite challenging. Various methods for attenuation correction exist, including model-based corrections using numerical ice-sheet models [52], [53] or 1-D analytic thermal models [27], [54], empirical bed echo-based corrections using along-track fitting [13] or 2-D cross-profile fitting [32], and englacial layer-based corrections based on the layers that are traced horizontally across profiles [30] or analyzed vertically as a function of depth [31]. All of these approaches by necessity make strong assumptions on glaciological conditions, and these assumptions have the potential to result in ambiguous or erroneous interpretations of basal conditions [26]. Therefore, direct observation, constraint, and correction of attenuation have the potential to reduce or remove the ambiguity between attenuation and basal conditions in radar sounding data.

Uncertainties in attenuation are dominated by uncertainties in englacial temperature, and corrections of attenuation in radar sounding data can be greatly improved with better constraints on englacial temperature. We show that for thermal profiles where typical radiometer-based retrievals work well, radiometers can provide these better englacial temperature constraints, improving attenuation corrections and thus, interpretations of basal conditions. For example, using the true temperature profile shown in Fig. 2(a), our simulation shows a radiometer can be used to estimate the temperature profile as a function of depth with relatively low median error, as depicted in Fig. 2(b). Using the retrieved temperature profiles with the model for attenuation in Section II-B produces attenuation estimates that have a median error of less than 1.5 dB across a broad frequency range [see Fig. 2(c) and (d)]. In cases where a radiometer is highly sensitive to emissions from the full depth of the ice column, the constraints provided for the radar attenuation from the radiometer instrument can be further improved.

Correcting for attenuation at this level on a nearly pulse-by-pulse basis with radiometer measurements could have a transformative impact on radar sounding analysis, enabling higher fidelity measurements of basal conditions and opening the door for true radiometric analysis of radar sounding data. This impact persists even in thermally complex areas where a fully radiometer-based temperature retrieval is not possible, as the combined constraint on englacial temperature (from a joint radar-radiometer, see Section V) still significantly reduces the ambiguity between attenuation and basal reflectivity. Furthermore, basal reflectivity signatures are relatively large, spanning a range of over 30 dB [52], [55], with spatial patterns of reflectivity (including roughness effects) spanning an even wider range [32]. The 25th–75th percentile error in Fig. 2(c) is approximately 15 dB for both frequencies, which still reduces uncertainty in basal reflectivity signatures to allow commentary on the thermal state of the bed (i.e., whether it is frozen or thawed). Thus when interpreting basal reflectivity patterns at the 10s of dB scale, the requirements placed on radiometer performance for attenuation correction are typically more easily met than those demanded the purpose of temperature retrievals.

V. Reducing Uncertainty in Model-Based Temperature Retrievals

While radiometers can sometimes provide significant constraints on englacial temperature profiles in regions where the assumptions of model-based retrievals hold [6], englacial temperature estimates from radiometer brightness temperatures alone are insufficient in many of the most dynamic, rapidly changing, and consequential portions of the ice sheet. Model-based retrievals inherently suffer degraded accuracy when the functional form of the a priori thermal model is incorrect or does not capture complex thermal behavior (e.g., temperate ice or non-steady state thermal regimes) [18]. Alternatively, exploiting the complementary sensitivity of a radar sounding instrument augments the radiometer's observational capabilities and lessens overall system demands by utilizing the radar, rather than a radiometer, to place constraints on the englacial temperature in areas of deep and warm ice. Here, we highlight the benefits radar data provides to radiometer-based thermal profile retrievals.

Active electromagnetic measurements of attenuation made by ice-penetrating radar sounders are highly complementary to the passive measurements of brightness temperature by microwave radiometers. Because the attenuation signal increases exponentially with temperature, it becomes easier for the radar to observe and discriminate this signal as the temperature of the ice increases. Fig. 3(g) and (h) demonstrates that improvement in englacial temperature observations on the order of 10 K, especially in deep/warm ice, can be achieved by adding a radar measurement of attenuation as compared to the radiometer measurements alone [see Fig. 3(b)–(d)]. Including a radar measurement of depth-integrated attenuation thus provides valuable, supporting data to a radiometer's measurement of temperature in these potentially important areas.

Although these examples utilized the Robin and Budd analytic models, the complementary constraints of radiometer brightness temperature and radar attenuation measurements can be similarly exploited to improve model-data assimilation schemes using numerical ice-sheet models, which are applicable to a much wider range of ice-sheet flow and thermal regimes.

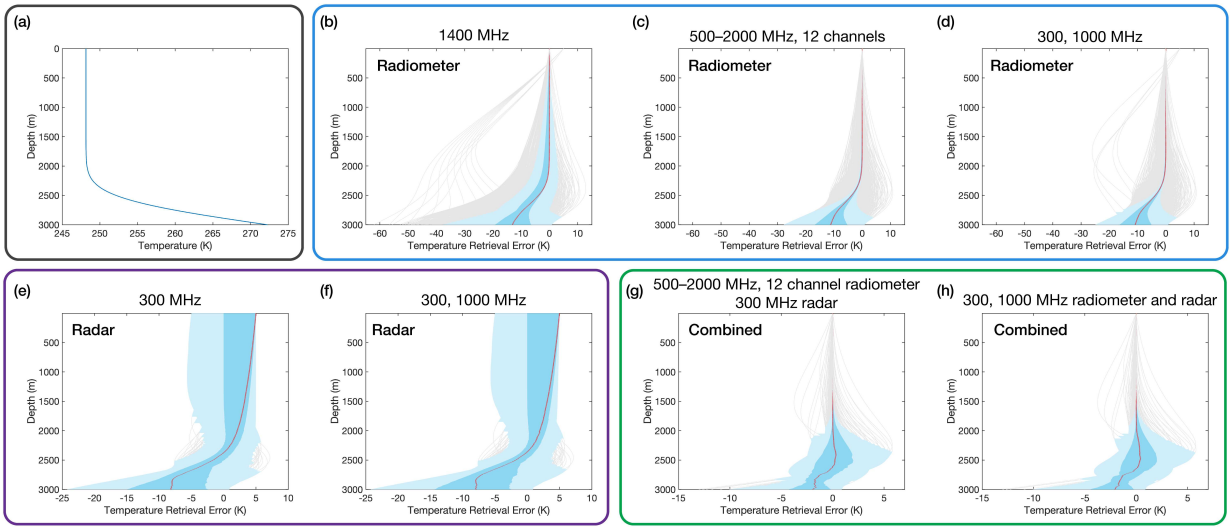

Fig. 3. Simulated temperature retrieval errors for a variety of system configurations measuring the true temperature profile in (a). Radiometer-only configurations are (b) 1400 MHz radiometer, (c) 12 channel wideband radiometer spanning 500–2000 MHz, and (d) dual channel radiometer at 300 and 1000 MHz. Radar-only configurations are (e) 300 MHz radar and (f) dual-frequency 300, 1000 MHz radar. Joint radar-radiometer configurations are (g) 12 channel wideband radiometer spanning 500–2000 MHz and a single-frequency 300 MHz radar, and (h) dual-frequency radar and radiometer, each with bands at 300 and 1000 MHz. All radiometers have ±1 K radiometric resolution. All radars have ±3 dB radiometric resolution.

VI. Architecture Implications

As shown above, an instrument that simultaneously collects radiometer and radarradiometer-only or radar sounding data has the potential to improve both microwave thermometry and basal condition observations across a range of ice-sheet thermal states. We now investigate potential factors in instrument design and architecture relevant for consideration when implementing such a system. Our particular interest in local-scale measurements of basal conditions and englacial thermal structure leads us to focus on a snowmobile-towed, ground-based solution. Although we focus on a ground-based solution and address the practicalities of building and operating such a system, the complementarity between active and passive microwave observations of ice-sheet thermal state and basal conditions also applies to airborne and satellite-borne systems. Our analysis of this approach suggests that combining SMOS or SMAP radiometer data at 1.4 GHz (the lowest frequencies available from spaceborne radiometers) over the ice sheets with radar data at roughly 300 MHz collected from various airborne radar campaigns is potentially promising for investigating ice-sheet thermal structure at the continent scale.

We discuss potential system architectures in the context of the simulated true temperature profile in Fig. 3(a), which requires a joint radar-radiometer system to obtain full top-to-bottom sensitivity to englacial temperature. The temperature profile in Fig. 3(a) is isothermal and relatively cold in the upper two-thirds of the ice column, with warming in the lower third of the column and a basal temperature that approaches the melting point. This profile is representative of thermal conditions near an ice divide with little to no horizontal advection and moderate accumulation. The presence of warm, deep ice prevents the radiometer from being sensitive to temperature at depth, while the relatively cold temperatures near the surface contribute relatively little to the total attenuation observed by the radar.

In Fig. 3(b)–(d), the temperature retrieval error is shown for three different radiometer-only system configurations, a single-frequency 1400 MHz radiometer [SMOS/SMAP analog, Fig. 3(b)], a 12 channel 500–2000 MHz radiometer [UWBRAD analog, Fig. 3(c)], and a dual-frequency 300 MHz/1000 MHz radiometer [see Fig. 3(d)]. All of these systems show similar behavior in the temperature retrieval, with generally good constraints in the upper portion of the ice column where the englacial temperature is cold and consistent, and increasing temperature error near the bed as the englacial temperature warms and the radiometers lose sensitivity. Fig. 3(e) and (f) shows the temperature retrieval error for two radar-only system configurations, a single-frequency 300 MHz radar, and a dual-frequency 300 MHz/1000 MHz radar. These results show greater error in the radar retrievals near the surface and less error near the bed, as expected based on the magnitude of the englacial temperature profile and attenuation as a function of depth.

Significantly improved constraints can be provided on the recovered temperature profile by using a joint radar-radiometer system. Fig. 3(g) and (h) shows the retrieved temperature error using two different system configurations for a joint radar-radiometer. In both joint system cases, the temperature error is less than in either the radiometer-only or radar-only case. Furthermore, the error remains relatively low throughout the entire depth of the ice column. Fig. 4 overlays the median temperature retrieval error for each system architecture and the simulated retrieval in Fig. 3. It is clear from this figure that the radiometer instrument provides important constraints on the englacial temperature in the upper portion of the ice column. The reduced error achieved by combining the radar and radiometer measurements shows that a joint system is more capable of observing and reproducing the full vertical structure of the englacial temperature profile.

Using the true temperature profile in Fig. 3(a) as an exemplar, we explore joint radar-radiometer system designs which maximize the amount of thermal data collected by the instrument while minimizing system complexity.

A. Channel Quantity and Spacing

A major design choice in the implementation of a joint microwave radar-radiometer is the center frequency, quantity,

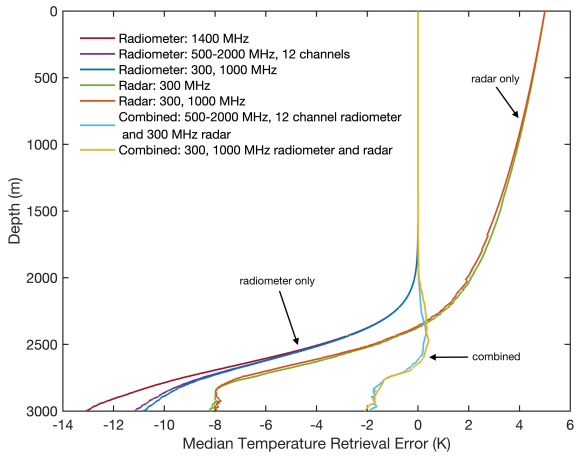

Fig. 4. Median temperature retrieval errors for the simulated retrievals shown in Fig. 3.

and spacing of different channels. Prior work in radiometry over ice sheets focuses on the need for a multi-frequency, very wide bandwidth radiometer system, with different frequencies used to reconstruct a depth-dependent temperature profile [15], [20]. Most ice-penetrating radars are designed with a focus on measuring topography beneath the ice sheets, which leads to system designs with high bandwidth, fine range resolution, and high transmit power [18]. In a joint radar-radiometer system that is focused on measuring and constraining englacial temperature, the overall complexity for each system can be reduced, making the implementation of each individual instrument more tractable.

Fig. 3(g) and (h), shows the temperature retrieval errors for our example temperature profile using two different joint radar-radiometer system configurations. The first, Fig. 3(g), shows a system that uses a UWBRAD-like multi-frequency, wideband radiometer alongside a single-frequency 300 MHz radar, while the second, Fig. 3(h) shows a system with both the radar and radiometer having two bands at 300 and 1000 MHz. These results show nearly identical errors in the temperature retrievals for these two joint systems, suggesting that by further decreasing the lowest radiometer measurement to 300 MHz (which is practical for a ground-based system), similar sensitivity to the ice-sheet thermal structure can be achieved. The addition of a second active radar channel at 1000 MHz also improves reconstructions by capturing an additional constraint on the attenuation, which is frequency-dependent at frequencies above 500 MHz (see Section II-B). As noted previously, scattering and density changes within the firn may play an important role in ice-sheet brightness temperature measurements, and including a higher frequency radar channel can support the measurement and correction of these near-surface effects.

A joint dual-frequency radar-radiometer system reduces overall system complexity, as the active and passive channels can share some front-end hardware (amplifiers, antennas, etc.), and because it is generally easier to design and build relatively narrowband RF components, as compared to very wideband ones. Provided one frequency is low enough (approximately 300 MHz) and the other is sufficiently high to capture shallow temperature variations and attenuation changes (approximately 1000 MHz), one can use such a system to produce reconstructions of englacial temperature as a function of depth.

A simultaneous advantage and challenge for multi-frequency, wideband radiometer systems is the presence of radio frequency interference (RFI). Because radiometers make very sensitive passive measurements, active RF sources within a range of their receivers cause saturation, masking the actual signals of interest. In wideband radiometers, the larger frequency range provides more overall data and flexibility, such that if one channel is corrupted by RFI, others may not be and may still collect useful data [56]. However, being wideband also presents a challenge because it is highly likely that somewhere across that bandwidth RFI will be present and degrade the data, requiring a variety of sophisticated RFI detection algorithms [56]. A narrowband system may be designed to be frequency agile and adjust its exact center frequency to avoid RFI as measured onsite for a given survey [57]. We envision implementing our system on a software-defined radio to enable this agility and allow the actual bands used in a specific deployment to be adjusted according to on-the-spot measurements of RFI.

B. Radiometric Resolution

Radiometric resolution quantifies an instrument's inherent uncertainty to received power. An instrument with better radiometric resolution (higher sensitivity, lower uncertainty) can better discriminate incident signals with small differences in energy, and as a result, may be able to better recover the underlying ice-sheet thermal signatures. Fig. 5 explores the design space of radiometric resolution, with radiometric resolutions ranging from a modest ± 3 dB for the radar to a much tighter ± 0.5 dB, and radiometer radiometric resolutions (also called noise equivalent delta temperature, NEDT), ranging from ± 1 to ± 0.2 K.

There are two main takeaways from these simulations. The first is that a joint radar-radiometer system with modest radiometric resolutions for each instrument [see Fig. 5(a)], still recovers the englacial temperature better than a highly precise radiometer-only system [see Fig. 5(i)]. Again, this is because the radar adds a complementary sensitivity to a temperature that is particularly evident in deep ice. An important implication of this result is that a joint system, with relaxed requirements on radiometric resolution, is much easier to implement than a single instrument with tight radiometric resolution.

The second takeaway from Fig. 5 is that while improving radiometric resolution in a joint radar-radiometer system does reduce the median error and spread in error of the recovered temperature, it does not do so significantly. Fig. 5(b) and (c), which have improved radiometric resolutions for the joint system, have fewer outliers and lower basal temperature error as compared to Fig. 5(a). However, there is not much difference between the ± 1 dB/± 0.5 K case and the ± 0.5 dB/± 0.2 K case, meaning additional improvements in radiometric resolution, which may require significantly increased system complexity, may not provide enough improvement in sensitivity to thermal structure to be justified. This suggests that a less complex and easier-to-implement joint radar-radiometer system may be sufficient to observe the englacial temperature in many cases.

C. Antenna Beamwidth and Polarization

Historically, radiometers have used rather directive antennas, while radar sounders have used nearly isotropic antennas.

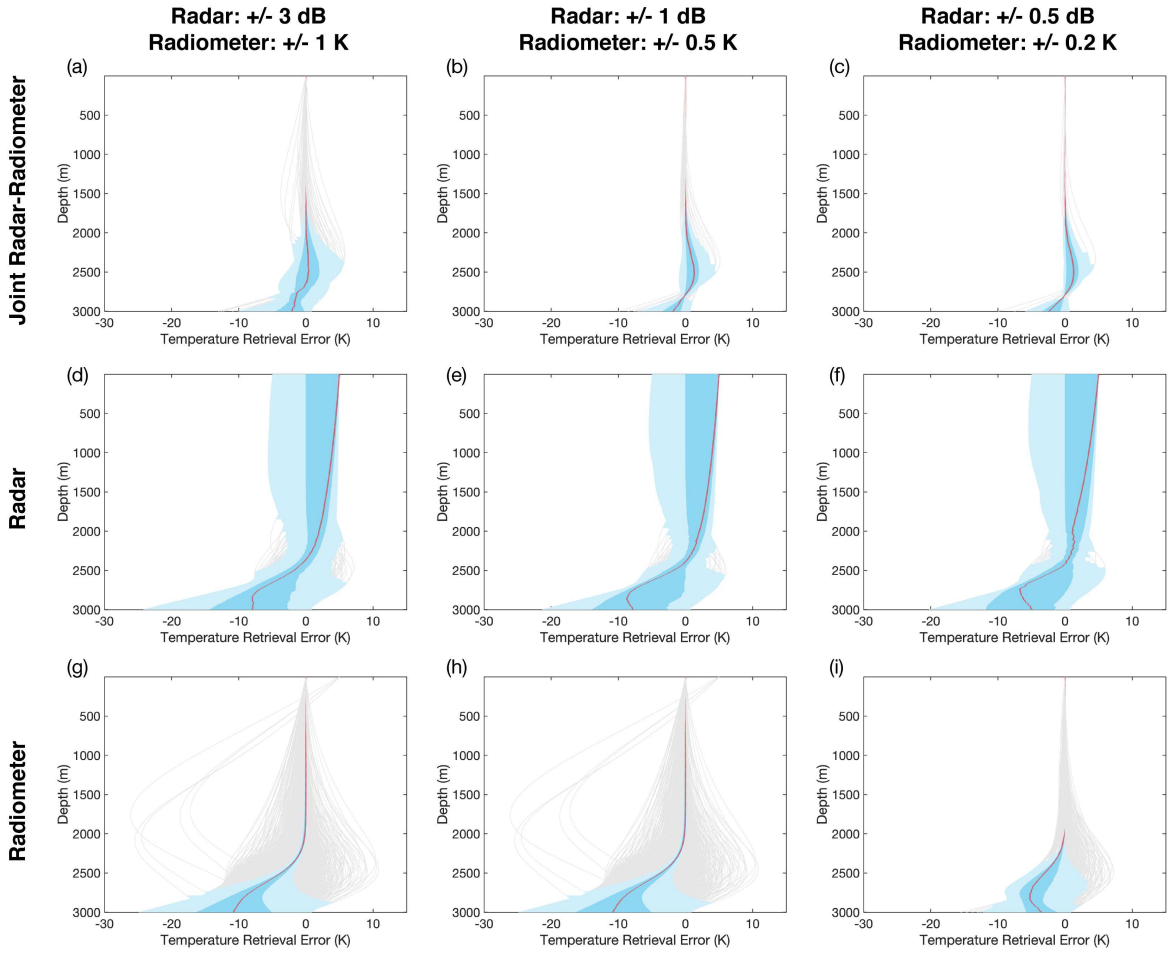

Fig. 5. Simulated temperature retrieval errors for a variety of system configurations measuring the true temperature profile in Fig. 3(a). (a)–(c) Joint radar-radiometer configurations, with a 300 and 1000 MHz radar and radiometer. (d)–(f) Radar-only configurations, with a 300 and 1000 MHz radar. (g)–(i) Radiometer-only configurations with a 300 and 1000 MHz radiometer. Columns show different radiometric resolutions, improving from left to right. (a), (d), and (g) ±3 dB radiometric resolution for the radar and ±1 K radiometric resolution for the radiometer. (b), (e), and (h) ±1 dB for the radar, ±0.5 K for the radiometer. (c), (f), and (i) ±0.5 dB for the radar, ±0.2 K for the radiometer.

Because we focus on a towed, ground-based system, we are able to use less directive antennas. Fig. 6 shows the impact of varying half power beamwidth (HPBW) for a ground-based radiometer. While improvement is seen in the radiometer-only configurations with narrowing HPBW in Fig. 6(a)–(c), the improvement is only marginal. More importantly, Fig. 6(d) shows that a joint radar-radiometer system with a nondirectional antenna can still more accurately recover the true temperature profile, despite limited antenna directivity. This shows again that by combining radar and radiometer instruments, we are able to reduce the overall complexity and requirements of each individual instrument. Reduced antenna directivity requirements are also advantageous in that smaller antenna sizes can be acceptable.

While we have used Fig. 3(a) as an exemplar true temperature profile for our discussion of system architecture, a dual-frequency joint radar-radiometer is advantageous across a wide range of true temperature profiles. Of the 358 667 temperature profiles simulated, in 270 798 profiles, a dual-frequency joint radar-radiometer (e.g., 300/1000 MHz, ±3 dB, ±1 K radiometric resolution, isotropic antenna) achieved median temperature retrieval error averaged over the full depth of the ice column less than or equal to the depth-averaged median temperature retrieval error of either individual instrument. The radiometer instrument alone achieved the same

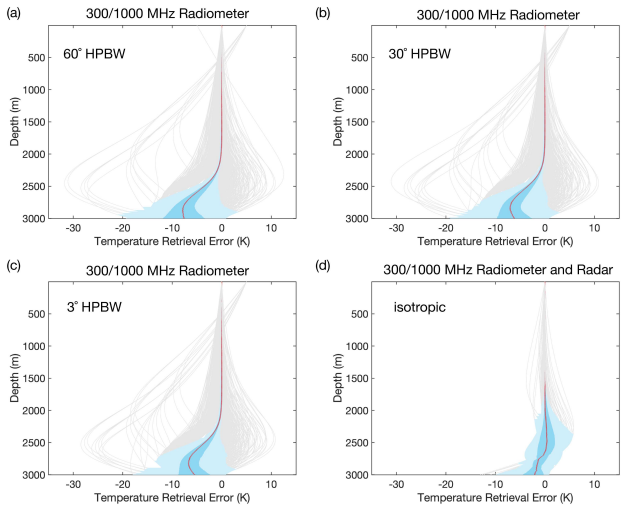

Fig. 6. Simulated temperature retrieval errors for a dual frequency 300, 1000 MHz radiometer measuring the true profile in Fig. 3(a), using (a) 60° HPBW antenna, (b) 30° HPBW antenna, and (c) 3° HPBW antenna. (d) Simulated temperature retrieval for a joint radar-radiometer system with channels at 300 and 1000 MHz and an isotropic antenna. All simulations have ±3 dB and ±1 K radiometric resolution for the radar and radiometer, respectively.

or lower depth-averaged median temperature retrieval errors than the radar or joint system in 226 214 profiles, and the

radar achieved the same or lower depth-averaged median temperature retrieval errors in 64 862 profiles. In practice, the performance metric of a system depends on the application and glaciological process being studied, and it is challenging to quantify performance without a specific application, but using the general metric above, it is clear that a joint radar-radiometer has potential use across many thermal profiles.

VII. Conclusion

Measuring ice-sheet thermal state is critical for answering a wide range of glaciological questions and for improving sea level projections from numerical ice-sheet models. Existing remote sensing techniques face significant challenges in recovering the full top-to-bottom thermal profile in ice sheets. We showed that the sensitivities of active and passive microwave measurements are highly complementary and that by combining active radar measurements of attenuation with passive radiometer measurements of brightness temperature, significantly improved top-to-bottom constraints on englacial temperature are achievable. Specifically, we showed that a ground-based joint radar-radiometer instrument can reduce requirements on channel quantity, radiometric resolution, and antenna beamwidth when compared to those for a radar or radiometer alone. The fundamental complementarity of radar and radiometer measurements and the framework for their joint analysis can also be extended to airborne or satellite systems. By combining active and passive microwave observations, we can improve our estimates of both the thermal state of ice sheets and the attenuation-corrected radar characterization of basal conditions in the most dynamic, compelling, and consequential portions of ice sheets and glaciers.

References

[1] W. F. Budd and T. H. Jacka, "A review of ice rheology for ice sheet modelling," *Cold Regions Sci. Technol.*, vol. 16, no. 2, pp. 107–144, Jul. 1989.

[2] M. Lüthi, M. Funk, A. Iken, S. Gogineni, and M. Truffer, "Mechanisms of fast flow in Jakobshavn isbræ, West Greenland: Part III. Measurements of ice deformation, temperature and cross-borehole conductivity in boreholes to the bedrock," *J. Glaciol.*, vol. 48, no. 162, pp. 369–385, 2002.

[3] P. Hunter, C. Meyer, B. Minchew, M. Haseloff, and A. Rempel, "Thermal controls on ice stream shear margins," *J. Glaciol.*, vol. 67, no. 263, pp. 435–449, Jun. 2021.

[4] J. Suckale, J. D. Platt, T. Perol, and J. R. Rice, "Deformation-induced melting in the margins of the West Antarctic ice streams," *J. Geophys. Res., Earth Surf.*, vol. 119, no. 5, pp. 1004–1025, May 2014.

[5] E. Larour, M. Morlighem, H. Seroussi, J. Schiermeier, and E. Rignot, "Ice flow sensitivity to geothermal heat flux of Pine Island Glacier, Antarctica," *J. Geophys. Res., Earth Surf.*, vol. 117, no. F4, pp. 1–12, 2012.

[6] S. Rezvanbehbahani, C. J. Veen, and L. A. Stearns, "An improved analytical solution for the temperature profile of ice sheets," *J. Geophys. Res., Earth Surf.*, vol. 124, no. 2, pp. 271–286, Feb. 2019.

[7] E. J. Dawson, D. M. Schroeder, W. Chu, E. Mantelli, and H. Seroussi, "Ice mass loss sensitivity to the Antarctic ice sheet basal thermal state," *Nature Commun.*, vol. 13, no. 1, pp. 1–9, Sep. 2022.

[8] E. Mantelli, M. Haseloff, and C. Schoof, "Ice sheet flow with thermally activated sliding. Part 1: The role of advection," *Proc. Roy. Soc. A, Math., Phys. Eng. Sci.*, vol. 475, no. 2230, Oct. 2019, Art. no. 20190410.

[9] A. T. Fisher, K. D. Mankoff, S. M. Tulaczyk, S. W. Tyler, and N. Foley, "High geothermal heat flux measured below the West Antarctic ice sheet," *Sci. Adv.*, vol. 1, no. 6, Jul. 2015, Art. no. e1500093.

[10] P. Neff, "A review of the brittle ice zone in polar ice cores," *Ann. Glaciol.*, vol. 55, no. 68, pp. 72–82, 2014.

[11] R. Mulvaney, J. Triest, and O. Alemany, "The James Ross island and the fletcher promontory ice-core drilling projects," *Ann. Glaciol.*, vol. 55, no. 68, pp. 179–188, 2014.

[12] R. Mulvaney et al., "Ice drilling on Skytrain ice rise and Sherman Island, Antarctica," *Ann. Glaciol.*, vol. 62, nos. 85–86, pp. 311–323, Sep. 2021.

[13] D. M. Schroeder, H. Seroussi, W. Chu, and D. A. Young, "Adaptively constraining radar attenuation and temperature across the Thwaites Glacier catchment using bed echoes," *J. Glaciol.*, vol. 62, no. 236, pp. 1075–1082, 2016.

[14] N. L. Bienert et al., "Post-processing synchronized bistatic radar for long offset glacier sounding," *IEEE Trans. Geosci. Remote Sens.*, vol. 60, 2022, Art. no. 1001917.

[15] C. Yardim et al., "Greenland ice sheet subsurface temperature estimation using ultrawideband microwave radiometry," *IEEE Trans. Geosci. Remote Sens.*, vol. 60, 2022, Art. no. 4300312.

[16] J. A. Dowdeswell and S. Evans, "Investigations of the form and flow of ice sheets and glaciers using radio-echo sounding," *Rep. Prog. Phys.*, vol. 67, no. 10, pp. 1821–1861, 2004.

[17] J. A. MacGregor, D. P. Winebrenner, H. Conway, K. Matsuoka, P. A. Mayewski, and G. D. Clow, "Modeling englacial radar attenuation at Siple Dome, West Antarctica, using ice chemistry and temperature data," *J. Geophys. Res.*, vol. 112, no. F3, pp. 1–14, 2007.

[18] D. M. Schroeder et al., "Five decades of radioglaciology," *Ann. Glaciol.*, vol. 61, no. 81, pp. 1–13, Apr. 2020.

[19] F. Ulaby and D. Long, *Microwave Radar and Radiometric Remote Sensing*. Norwood, MA, USA: Artech House, 2015.

[20] K. C. Jezek et al., "Radiometric approach for estimating relative changes in intraglacier average temperature," *IEEE Trans. Geosci. Remote Sens.*, vol. 53, no. 1, pp. 134–143, Jan. 2014.

[21] G. Macelloni, M. Leduc-Leballeur, F. Montomoli, M. Brogioni, C. Ritz, and G. Picard, "On the retrieval of internal temperature of Antarctica ice sheet by using SMOS observations," *Remote Sens. Environ.*, vol. 233, Nov. 2019, Art. no. 111405.

[22] J. Z. Miller, R. Culberg, D. G. Long, C. A. Shuman, D. M. Schroeder, and M. J. Brodzik, "An empirical algorithm to map perennial firn aquifers and ice slabs within the Greenland ice sheet using satellite L-band microwave radiometry," *Cryosphere*, vol. 16, no. 1, pp. 103–125, Jan. 2022.

[23] M. J. Andrews et al., "The ultrawideband software-defined microwave radiometer: Instrument description and initial campaign results," *IEEE Trans. Geosci. Remote Sens.*, vol. 56, no. 10, pp. 5923–5935, Oct. 2018.

[24] C. Mätzler, "Microwave dielectric properties of ice," in *Thermal Microwave Radiation: Applications for Remote Sensing*. Edison, NJ, USA: IET, vol. 52, 2006, pp. 455–462.

[25] A. L. Broome and D. M. Schroeder, "A radiometrically precise multi-frequency ice-penetrating radar architecture," *IEEE Trans. Geosci. Remote Sens.*, vol. 60, 2022, Art. no. 5104515.

[26] K. Matsuoka, "Pitfalls in radar diagnosis of ice-sheet bed conditions: Lessons from englacial attenuation models," *Geophys. Res. Lett.*, vol. 38, no. 5, pp. 1–12, Mar. 2011.

[27] A. Ilisei, J. Li, S. Gogineni, and L. Bruzzone, "Estimation of ice sheet attenuation by using radar sounder and ice core data," *Proc. SPIE*, vol. 10004, Oct. 2016, Art. no. 1000416.

[28] K. Matsuoka, J. A. MacGregor, and F. Pattyn, "Predicting radar attenuation within the Antarctic ice sheet," *Earth Planet. Sci. Lett.*, vols. 359–360, pp. 173–183, Dec. 2012.

[29] W. Chu, D. M. Schroeder, H. Seroussi, T. T. Creyts, and R. E. Bell, "Complex basal thermal transition near the onset of Petermann Glacier, Greenland," *J. Geophys. Res., Earth Surf.*, vol. 123, no. 5, pp. 985–995, 2018.

[30] J. A. MacGregor et al., "Radar attenuation and temperature within the Greenland ice sheet," *J. Geophys. Res., Earth Surf.*, vol. 120, no. 6, pp. 983–1008, 2015.

[31] B. H. Hills, K. Christianson, and N. Holschuh, "A framework for attenuation method selection evaluated with ice-penetrating radar data at South Pole Lake," *Ann. Glaciol.*, vol. 61, no. 81, pp. 176–187, Apr. 2020.

[32] W. Chu et al., "Multisystem synthesis of radar sounding observations of the Amundsen Sea sector from the 2004–2005 field season," *J. Geophys. Res., Earth Surf.*, vol. 126, no. 10, p. e2021JF006296, Oct. 2021.

[33] W. Chu, D. M. Schroeder, and M. R. Siegfried, "Retrieval of englacial firn aquifer thickness from ice-penetrating radar sounding in southeastern Greenland," *Geophys. Res. Lett.*, vol. 45, no. 21, p. 11, Nov. 2018.

[34] D. P. Winebrenner, P. M. S. Kintner, and J. A. MacGregor, "New estimates of ice and oxygen fluxes across the entire lid of Lake Vostok from observations of englacial radio wave attenuation," *J. Geophys. Res., Earth Surf.*, vol. 124, no. 3, pp. 795–811, Mar. 2019.

[35] K. Cuffey and W. Paterson, *The Physics of Glaciers*. New York, NY, USA: Academic, 2010.

[36] K. C. Jezek, C. Yardim, J. T. Johnson, G. Macelloni, and M. Brogioni, "Analysis of ice-sheet temperature profiles from low-frequency airborne remote sensing," *J. Glaciol.*, vol. 2022, pp. 1–11, Mar. 2022.

[37] T. A. Scambos et al., "How much, how fast? A science review and outlook for research on the instability of Antarctica's Thwaites glacier in the 21st century," *Global Planet. Change*, vol. 153, pp. 16–34, Jun. 2017.

[38] W. Budd, D. Jenssen, and U. Radok, *Derived Physical Characteristics of the Antarctic Ice Sheet: Mark I*. Melbourne, VIC, Australia: University of Melbourne, 1971.

[39] E. Larour, H. Seroussi, M. Morlighem, and E. Rignot, "Continental scale, high order, high spatial resolution, ice sheet modeling using the ice sheet system model (ISSM)," *J. Geophys. Res., Earth Surf.*, vol. 117, no. F1, pp. 1–20, 2012.

[40] C. R. Meyer and B. M. Minchew, "Temperate ice in the shear margins of the Antarctic ice sheet: Controlling processes and preliminary locations," *Earth Planet. Sci. Lett.*, vol. 498, pp. 17–26, Sep. 2018.

[41] F. Ulaby, R. Moore, and A. Fung, *Microwave Remote Sensing: Active and Passive*, vol. 1. Norwood, MA, USA: Artech House, 1982.

[42] R. L. Hooke, *Principles of Glacier Mechanics*. Cambridge, U.K.: Cambridge Univ. Press, 2019.

[43] A. L. Broome, D. M. Schroeder, and J. T. Johnson, "Measuring englacial temperatures with a combined radar-radiometer," in *Proc. IEEE Int. Geosci. Remote Sens. Symp.*, Jul. 2021, pp. 2947–2950.

[44] S. Tan et al., "Physical models of layered polar firn brightness temperatures from 0.5 to 2 GHz," *IEEE J. Sel. Topics Appl. Earth Observ. Remote Sens.*, vol. 8, no. 7, pp. 3681–3691, Jul. 2015.

[45] H. Xu et al., "Polar firn properties in Greenland and Antarctica and related effects on microwave brightness temperatures," *EGUsphere*, vol. 2022, pp. 1–27, Jan. 2022.

[46] M. Brogioni, G. Macelloni, F. Montomoli, and K. C. Jezek, "Simulating multifrequency ground-based radiometric measurements at Dome C—Antarctica," *IEEE J. Sel. Topics Appl. Earth Observ. Remote Sens.*, vol. 8, no. 9, pp. 4405–4417, Sep. 2015.

[47] K. C. Jezek et al., "500–2000-MHz brightness temperature spectra of the northwestern Greenland ice sheet," *IEEE Trans. Geosci. Remote Sens.*, vol. 56, no. 3, pp. 1485–1496, Mar. 2018.

[48] R. Culberg and D. Schroeder, "Firn clutter constraints on the design and performance of orbital radar ice sounders," *IEEE Trans. Geosci. Remote Sens.*, vol. 58, no. 9, pp. 1–18, Sep. 2020.

[49] D. Bai, X. Dong, S. Tjuatja, and D. Zhu, "An improved combined active and passive remote sensing approach for ICE sheet internal temperature profiling," in *Proc. IEEE Int. Geosci. Remote Sens. Symp.*, Jul. 2022, pp. 3896–3899.

[50] E. van Meijgaard et al., *The KNMI Regional Atmospheric Climate Model RACMO, Version 2.1*. De Bilt, The Netherlands: KNMI, 2008.

[51] K. Jezek et al., "Remote sensing of sea ice thickness and salinity with 0.5–2 GHz microwave radiometry," *IEEE Trans. Geosci. Remote Sens.*, vol. 57, no. 11, pp. 1–13, Nov. 2019.

[52] K. Christianson et al., "Basal conditions at the grounding zone of Whillans ice stream, West Antarctica, from ice-penetrating radar," *J. Geophys. Res., Earth. Surf.*, vol. 121, no. 11, pp. 1954–1983, 2016.

[53] S. P. Carter, D. D. Blankenship, D. A. Young, and J. W. Holt, "Using radar-sounding data to identify the distribution and sources of subglacial water: Application to Dome C, East Antarctica," *J. Glaciol.*, vol. 55, no. 194, pp. 1025–1040, 2009.

[54] M. E. Peters, D. D. Blankenship, S. P. Carter, S. D. Kempf, D. A. Young, and J. W. Holt, "Along-track focusing of airborne radar sounding data from West Antarctica for improving basal reflection analysis and layer detection," *IEEE Trans. Geosci. Remote Sens.*, vol. 45, no. 9, pp. 2725–2736, Sep. 2007.

[55] M. E. Peters, "Analysis techniques for coherent airborne radar sounding: Application to West Antarctic ice streams," *J. Geophys. Res.*, vol. 110, no. B6, pp. 1–17, 2005.

[56] M. J. Andrews, J. T. Johnson, M. Brogioni, G. Macelloni, and K. C. Jezek, "Properties of the 500–2000-MHz RFI environment observed in high-latitude airborne radiometer measurements," *IEEE Trans. Geosci. Remote Sens.*, vol. 60, 2022, Art. no. 5301311.

[57] S. Peters, D. Schroeder, D. Castelletti, M. Haynes, and A. Romero-Wolf, "In situ demonstration of a passive radio sounding approach using the sun for echo detection," *IEEE Trans. Geosci. Remote Sens.*, vol. 56, no. 12, pp. 7338–7349, Jul. 2018.

Anna L. Broome (Graduate Student Member, IEEE) received the B.S.E. degree (magna cum laude) in electrical engineering from Princeton University, Princeton, NJ, USA, in 2018, and the M.S. degree in electrical engineering from Stanford University, Stanford, CA, USA, in 2020, where she is currently pursuing the Ph.D. degree in electrical engineering with a focus on developing radiometrically optimized radar sounding systems for characterizing ice sheet basal conditions.

She is currently a member of the Stanford Radio Glaciology Laboratory, the Department of Geophysics, and the Department of Electrical Engineering, Stanford University, advised by Prof. Dustin M. Schroeder.

Ms. Broome has received the U.S. Department of Defense National Defense Science and Engineering Graduate Fellowship and the Stanford Enhancing Diversity in Graduate Education Fellowship.

Dustin M. Schroeder (Senior Member, IEEE) received the B.A. degree in physics and the B.S.E.E. degree (magna cum laude) in electrical engineering from Bucknell University, Lewisburg, PA, USA, in 2007, and the Ph.D. degree in geophysics from The University of Texas at Austin, Austin, TX, USA, in 2014.

He is currently an Associate Professor of geophysics and electrical engineering with Stanford University, Stanford, CA, USA, where he is also a Senior Fellow with the Stanford Woods Institute for the Environment. His research group seeks to approach problems from both an Earth system science and radar system engineering perspective. He has participated in three Antarctic field seasons with the Investigating the Cryospheric Evolution of the Central Antarctic Plate (ICECAP) Project and NASA's Operation Ice Bridge, as a Radar Engineer and an Operator. His research interests include observing and understanding the role that subglacial water plays in the evolution and stability of continental ice sheets and its contribution to the rate of sea level rise, and also include the development, use, and analysis of geophysical radar remote sensing systems that are optimized to observe hypothesis-specific phenomena.

Dr. Schroeder is a Science Team Member on the Radar for Europa Assessment and Sounding: Ocean to Near-Surface (REASON) Instrument on NASA's Europa Clipper Mission and the Mini-RF Instrument on NASA's Lunar Reconnaissance Orbiter.

Joel T. Johnson (Fellow, IEEE) received the bachelor's degree in electrical engineering from the Georgia Institute of Technology, Atlanta, GA, USA, in 1991, and the S.M. and Ph.D. degrees from the Massachusetts Institute of Technology, Cambridge, MA, USA, in 1993 and 1996, respectively.

He is currently the Burn and Sue Lin Professor of the Department of Electrical and Computer Engineering and the ElectroScience Laboratory, The Ohio State University, Columbus, OH, USA. His research interests are in the areas of microwave remote sensing, propagation, and electromagnetic wave theory.

Dr. Johnson is a member of Commissions B and F of the International Union of Radio Science (URSI), Tau Beta Pi, Eta Kappa Nu, and Phi Kappa Phi. He has received the 1993 Best Paper Award from the IEEE Geoscience and Remote Sensing Society. He was named as an Office of Naval Research Young Investigator, National Science Foundation Career Awardee, and Presidential Early Career Award for Scientists and Engineers (PECASE) Award Recipient in 1997. He was recognized by the U.S. National Committee of URSI as a Booker Fellow in 2002.